

Article

Optical “Blinking” Triggered by Collisions of Single Supramolecular Assemblies of Amphiphilic Molecules with Interfaces of Liquid Crystals

Michael Tsuei, Manisha Shivrayan, Young-Ki Kim, Sankaran Thayumanavan, and Nicholas L. Abbott

J. Am. Chem. Soc., **Just Accepted Manuscript** • DOI: 10.1021/jacs.9b13360 • Publication Date (Web): 21 Feb 2020

Downloaded from pubs.acs.org on February 22, 2020

Just Accepted

“Just Accepted” manuscripts have been peer-reviewed and accepted for publication. They are posted online prior to technical editing, formatting for publication and author proofing. The American Chemical Society provides “Just Accepted” as a service to the research community to expedite the dissemination of scientific material as soon as possible after acceptance. “Just Accepted” manuscripts appear in full in PDF format accompanied by an HTML abstract. “Just Accepted” manuscripts have been fully peer reviewed, but should not be considered the official version of record. They are citable by the Digital Object Identifier (DOI®). “Just Accepted” is an optional service offered to authors. Therefore, the “Just Accepted” Web site may not include all articles that will be published in the journal. After a manuscript is technically edited and formatted, it will be removed from the “Just Accepted” Web site and published as an ASAP article. Note that technical editing may introduce minor changes to the manuscript text and/or graphics which could affect content, and all legal disclaimers and ethical guidelines that apply to the journal pertain. ACS cannot be held responsible for errors or consequences arising from the use of information contained in these “Just Accepted” manuscripts.

Optical “Blinking” Triggered by Collisions of Single Supramolecular Assemblies of Amphiphilic Molecules with Interfaces of Liquid Crystals

Michael Tsuei[†], Manisha Shivrayan^{2†}, Young-Ki Kim¹, S. Thayumanavan^{2*}, and Nicholas L. Abbott^{1*}

¹ Smith School of Chemical and Biomolecular Engineering, Cornell University, Ithaca, NY 14853, USA

² Department of Chemistry, University of Massachusetts Amherst, Amherst, MA 01003, USA

ABSTRACT: We report that incubation of aqueous dispersions of supramolecular assemblies formed by synthetic alkyl triazole-based amphiphiles against interfaces of thermotropic liquid crystals (LCs; 4-cyano-4'-pentylbiphenyl) triggers spatially localized (micrometer-scale) and transient (sub-second) flashes of light to be transmitted through the LC. Analysis of the spatio-temporal response of the LC supports our proposal that each optical “blinking” event results from collision of a single supramolecular assembly with the LC interface. Particle tracking at the LC interface confirmed that collision and subsequent spreading of amphiphiles at the interface generates a surface pressure-driven interfacial flow (Marangoni flow) that causes transient reorientation of LC and generation of a bright optical flash between crossed polarizers. We also found that dispersions of phospholipid vesicles cause “blinks”. When using vesicles formed from 1,2-dilauroyl-sn-glycero-3-phosphocholine (DLPC), we measured the frequency of blinking to decrease proportionally with the number density of vesicles in the aqueous phase, consistent with single vesicle events, with the lifetime of each blink dependent on vesicle size (800 ± 80 nm to 150 ± 30 nm). For 100 μ M of DLPC, we measured vesicles with a diameter of 940 ± 290 nm to generate 47 ± 9 blinks $\text{min}^{-1} \text{mm}^{-2}$, revealing that the fraction of vesicle collisions resulting in fusion with the LC interface is $\sim 10^{-3}$. Overall, the results in this paper unmask new non-equilibrium behaviors of amphiphiles at LC interfaces, and provide fresh approaches for exploring the dynamic interactions of supramolecular assemblies of amphiphiles with fluid interfaces at the single-event level.

INTRODUCTION

Dynamic interactions of amphiphilic assemblies, including vesicles, at biological interfaces underlie processes as diverse as transmission of synaptic signals,¹ blebbing of microvesicles from cells for intercellular communication²⁻³ and endocytosis.⁴ Key aspects of these processes have been recapitulated using synthetic amphiphiles, such as the fusion of vesicles into monolayers⁵ or bilayers at surfaces of solids.⁶⁻⁸ In this paper, we report the observation that interfaces of water-immiscible liquid crystals (LCs), when incubated against aqueous dispersions of synthetic and biological amphiphiles and viewed using crossed-polarizers (transmission mode), exhibit transient bright domains. We establish that the “blinking” events arise from non-equilibrium states of the LC caused by dynamic interactions of the LC with single supramolecular assemblies formed by the amphiphiles (including vesicles).

The LCs used in our study are formed from 4-cyano-4'-pentylbiphenyl (5CB) (Scheme 1a). As a single component at room temperature, 5CB forms a liquid within which the 5CB molecules exhibit long-range orientational order (a so-called nematic LC phase).⁹⁻¹⁰ The long-range ordering of molecules within LCs gives rise to anisotropic properties

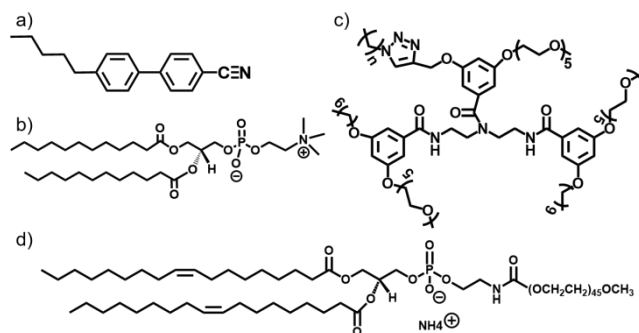
such as optical birefringence and elasticity, and enables LCs to amplify and transduce molecular-level events at interfaces into easily visualized and quantifiable changes in optical signals.¹¹⁻¹⁴ These characteristics have made LCs exemplary materials for reporting a range of molecular stimuli and events, including photo isomerizations,¹⁵⁻²⁰ enzymatic reactions,²¹ formation of DNA complexes,²² directed assembly of oligopeptides²³⁻²⁴ and interfacial interactions of ions.²⁵⁻²⁶

Of relevance to the study reported herein, a number of past studies of LCs have focused on understanding the equilibrium orientations of LCs at aqueous interfaces decorated by amphiphiles such as phospholipids (1,2-dilauroyl-sn-glycerol-3-phosphocholine (DLPC), Scheme 1b),^{12, 24, 27-28} synthetic surfactants (e.g. dodecyltrimethylammonium bromide (DTAB))^{11-12, 29-31} or peptide-polymer amphiphiles.^{21, 32} Adsorption of these amphiphiles from aqueous dispersions results in reorientation of the LCs in a manner that is dependent on the structure and the concentration of the amphiphiles.^{13, 29, 33-35} Various factors have been identified to influence the orientations of LCs at amphiphilic-decorated aqueous interfaces, including interdigitation of the aliphatic tails of the amphiphiles into the LCs,^{11-15, 27-28, 32-33} disorder induced

in the LCs due to frustrated packing of mesogens at the interface^{32, 36} and electrical double layer interactions.^{26, 37}

In this paper, we move beyond prior studies of the equilibrium properties of amphiphile-decorated LC interfaces to explore non-equilibrium states induced by dynamic interactions of amphiphilic assemblies. As noted above, this investigation was motivated by the observation of transient flashes of light transmitted through LC interfaces contacting aqueous solutions of alkyl-triazole oligomers (O₁, Scheme 1c) that we were studying to develop structure-property relationships for branched amphiphilic oligomers at LC interfaces. Scheme 1c shows the structure of the oligomer, which includes three design motifs; alkyl chains, oligoethylene glycol and a triazole ring. The alkyl chains facilitate anchoring of O₁ on the LC interface and the oligoethylene glycol moieties were used as hydrophilic arms to promote solubility of O₁ in aqueous solutions. The triazole ring, which was incorporated as part of the synthetic strategy, also increases the rigidity of O₁ and introduces asymmetry that impacts the organization of the amphiphiles at LC interfaces. Ongoing studies are addressing the effects of oligomer rigidity on LC ordering and will be reported elsewhere.

Subsequent to our initial observations with O₁, we found that optical blinking occurred with other amphiphilic systems (e.g. phospholipids). Our results reveal that the non-equilibrium states of the LC are generated by collisions of single amphiphilic assemblies with the LC interface, leading to transient interfacial flows that reorient the LCs.³⁸⁻³⁹ The results presented in this paper hint at broad utility of this phenomenon for probing the presence and properties of amphiphilic assemblies. Specifically, the approach enables characterization of interfacial events triggered by individual assemblies rather than large populations of assemblies,⁴⁰⁻⁴¹ does not require use of fluorescent labels (or other molecular probes)⁴⁰ and exploits unique attributes of LC interfaces, such as the high mobility necessary to observe Marangoni phenomena (in contrast to solid-supported amphiphile assemblies).⁴²⁻⁴³



Scheme 1: Molecular structures of a) 4-cyano-4'-pentylbiphenyl (5CB), b) 1,2-dilauroyl-sn-glycerol-3-phosphocholine (DLPC), c) amphiphilic branched oligomer (O₁) containing alkyl-triazole ($n = 13$) and pentaethylene glycol domains and d) PEGylated lipid (DOPE-PEG).

RESULTS AND DISCUSSION

LC Ordering Transitions Induced by O₁. In our initial experiments, films of LC were hosted within 20 μm -thick metal grids supported on dimethyloctadecyl[3-(trimethoxysilyl)propyl]ammonium chloride (DMOAP)-treated glass microscope slides (which orient nematic 5CB along the surface normal (Fig. 1a)) and then submerged into aqueous 10 mM phosphate-buffered saline (PBS) containing 25 μM O₁ (Fig. 1a-f). When viewed through crossed polarizers in transmission mode, the LC films initially exhibited a bright optical appearance with dark brushes (Schlieren texture), indicative of tangential LC alignment at the aqueous interface (planar anchoring; Fig. 1a,b). Subsequently, the LC displayed a time-dependent progression of interference colors with retardance values of 1400 ± 70 nm (0 min, Fig. 1b), 650 ± 210 nm (20 min, Fig. 1c), 300 ± 140 nm (40 min, Fig. 1d) and 0 nm (60 min, Fig. 1e). The progression of retardance values is consistent with a continuous tilting of the LC at the aqueous interface, from planar to perpendicular (homeotropic) anchoring (Fig. 1b-e) with increasing time. The end point of the continuous transition is a dark optical state, corresponding to homeotropic anchoring of the LC (Fig. 1e,f). Overall, these observations are consistent with spontaneous adsorption of O₁ onto the LC interface, triggering the reorientation of the LC. We also used LC films supported on polyimide-coated glass substrates that caused planar anchoring of LC. When these LC films were immersed in 25 μM O₁ in PBS, the LCs also underwent orientational transitions, indicating that adsorption of O₁ causes a change in the lowest free energy orientation (so-called easy axis) of the LC at the aqueous-LC interface (see Section S1).^{12-13, 15, 32, 44}

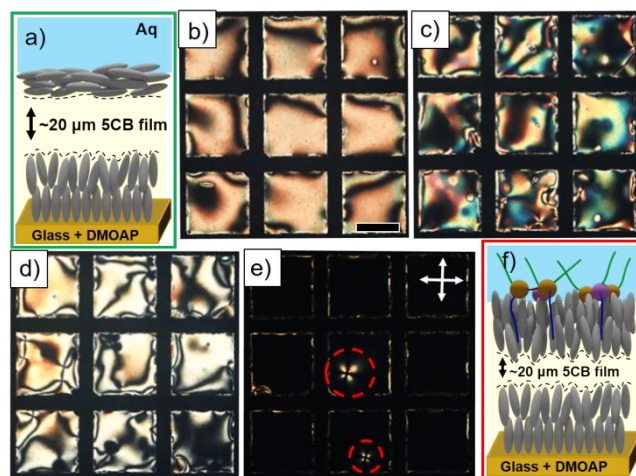


Figure 1: a,f) Schematic illustrations (side view) and b,e) corresponding micrographs (top view, crossed polarizers) of aqueous-LC interface exhibiting a,b) planar and e,f) homeotropic anchoring of LCs with respect to the aqueous-LC interface upon adsorption of O₁. b-e) Sequential micrographs (top view, crossed polarizers) of the LC interface after b) 0, c) 20, d) 40 and e) 60 min of contact with the aqueous O₁ solution (25 μM). Scale bar is 200 μm .

We compared the duration of the dynamic anchoring transition (60 ± 30 min at 25 μM of O₁) to the time required for diffusion of O₁ assemblies from the bulk aqueous phase

to the LC interface (50 min; using an experimentally measured diffusivity of $3.7 \times 10^{-13} \text{ m}^2/\text{s}$; see Section S2) and determined that the dynamics of the anchoring transition are controlled by diffusion of O_1 to the LC interface. Surprisingly, however, after the LC had transitioned to the homeotropic orientation, we observed localized (micrometer-scale) and transient (sub-second) flashes of light at the LC interface when viewed between crossed polarizers (transmission mode) (Fig. 1e, red circles, Video S1). Below we refer to the transient flashes of light as “blinking”. For an aqueous phase containing $25 \mu\text{M}$ of O_1 , directly following the observation of homeotropic anchoring, we measured $45 \pm 4 \text{ blinks min}^{-1} \text{ mm}^{-2}$ of LC interface.

Characterization of Blinking Events At LC Interfaces. Additional optical microscopy performed at high magnification led to four key observations regarding the blinking events. First, when viewed between crossed polarizers, blinking events generated transient Maltese crosses (Fig. 2a-d). This observation suggested that the blink was generated by a radially symmetric rotation of the LC orientation away from the surface normal (Fig. 2e inset). This interpretation was supported by measurement of the optical retardance of the LC during the blink and calculation of the angular rotation of the orientation of the LC away from the surface normal (tilt angle of the LC).^{10, 45} By assuming the LC tilt angle within the film to be dominated by the elastic energy of the LC, we estimate the average tilt angle of the LC (see Section S3) during the blinking event in Fig. 2b to be $\theta_{\text{avg}} \sim 23 \pm 4^\circ$ (see below and Section S9 for a more detailed model of the LC tilt).

Second, we quantified the temporal and spatial characteristics of individual blinks by analyzing the intensity of light transmitted through a single $285 \mu\text{m} \times 285 \mu\text{m}$ area of the LC interface. We found that the lifetime of a blink was typically subsecond but that it varied from one event to the next (Fig. 2f). The mean size of the footprint of the blink was $\sim 100 \mu\text{m}$, but it varied substantially between events (from $20 \mu\text{m}$ to $250 \mu\text{m}$, Fig. 2g). While individual blinking events were transient, we observed the blinking phenomena to persist at LC interfaces in contact with dispersions of O_1 for hours.

Third, when using bright field microscopy (no polarizers), we observed that a small fraction of blinks were preceded by the presence of micrometer-sized particles near the site of the blink. The particles were observed to disappear from the field of view during the blink (see Section S4). The majority of blinks, however, occurred in the absence of visible particles (Fig. 2h-k). These observations revealed that micrometer-sized particles can lead to, but were not required for, the generation of the blinks. The particles were not observed between crossed polarizers, indicating that they are not LC droplets. When combined, these observations led us to the hypothesis that the particles were O_1 aggregates and that blinking was a consequence of the interaction of O_1 aggregates (the majority of which are too small to be imaged) with the LC interface. Below, we explore this proposal.

Fourth, subsequent to our observations of blinking in homeotropically oriented samples, closer examination of LC samples that had not yet transitioned to the homeotropic orientation revealed evidence of blinks with footprints and durations similar to those observed in homeotropically aligned samples (see Section S5 for images and additional description).

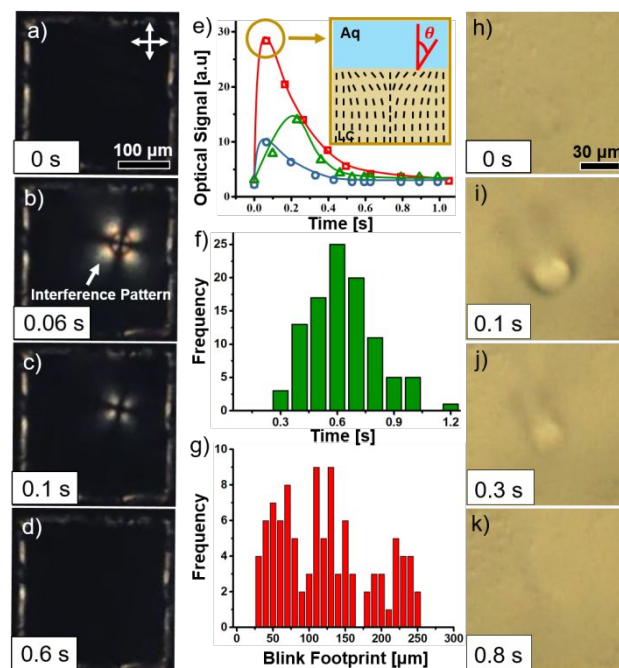


Figure 2: a-d) Sequential micrographs (crossed polarizers, top view) of a single blinking event at the LC interface contacting an aqueous O_1 solution ($C_{O_1} = 25 \mu\text{M}$). e) Corresponding transmittance profiles (red, green, blue) representing the intensity of light transmitted through the grid squares during three individual blinking events. Lines are drawn to guide the eye. Inset illustrates the director profile (side view) across the LC film during a blinking event. f) histogram of blinking lifetimes ($n=100$, bin size: 0.1 s). g) histogram of blinking footprint ($n=100$, bin size: $10 \mu\text{m}$). h-k) Sequential micrographs (bright field) of a single blinking event at the LC interface in contact with aqueous O_1 ($C_{O_1} = 25 \mu\text{M}$).

Correlation Between LC Blinking and Concentration of O_1 in the Aqueous Phase. We determined that blinking ceased when the aqueous dispersion of O_1 in contact with the LC was replaced by PBS free of O_1 (see Section S6). This result indicates that blinking requires the presence of O_1 in the bulk aqueous phase. Furthermore, after 48 hrs of contact with PBS free of O_1 , the LC remained in the homeotropic orientation, indicating slow desorption of O_1 from the LC interface at surface concentrations of O_1 that sustain homeotropic anchoring (see below for evidence of desorption of O_1).

We varied the concentration (0 - $25 \mu\text{M}$) of O_1 incubated against the LC and documented the blinking frequencies after 1 hour of incubation (Fig. 3a). Below a threshold concentration of $1 \mu\text{M}$ O_1 , no blinking was observed. Above the threshold, we measured the blinking frequency to increase in an approximately sigmoidal manner as a function of O_1 concentration (Fig. 3a). We hypothesized that the concentration-dependent frequency of blinking

shown in Fig. 3a was related to the concentration of O1 assemblies in the aqueous dispersions and thus frequency of collisions of O1 assemblies with the LC interface. By using dynamic light scattering, however, we found that the average sizes of the assemblies formed by O1 increased from ~100 nm to ~1000 nm (Fig. 3b, see Section S7) with concentration of O1 in the bulk aqueous solution. This result led us to conclude that the concentration-dependence of the blinking frequency reported in Fig. 3a likely reflects changes in both the number and size of O1 assemblies in the PBS.

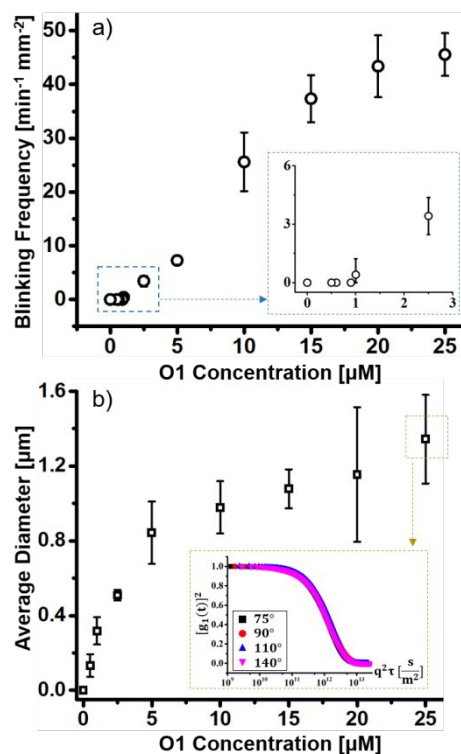


Figure 3: a) Blinking frequency at different concentrations of O1 in the aqueous solution. Inset shows a magnified plot at low O1 concentrations. b) O1 aggregate number average diameters with respect to O1 concentration in the aqueous solution. Inset shows autocorrelation functions using light scattering angles of 75°, 90°, 110° and 140° for aqueous solutions containing 25 μM O1 incubated for 4 hours at 25 °C. a,b) Data points show mean values and the error bars represent 1 standard deviation (n=3).

As an additional test of the connection between blinking and O1 aggregate size, we added urea to change the size and properties of O1 aggregates⁴⁶⁻⁴⁸ (see Section S8). Dynamic light scattering measurements conducted using 25 μM O1 in 8 M urea revealed that urea caused the size of O1 assemblies to decrease sixfold to 250 nm ± 180 nm. Upon submerging a LC film into an aqueous solution containing 8 M urea and 25 μM O1, blinking ceased, but the anchoring of the LC changed from planar to homeotropic, consistent with adsorption of O1 onto the LC interface. A control experiment performed with 8 M urea in the absence of O1 did not trigger an anchoring transition or blinking of the LC. These results support our hypothesis that the size of O1 assemblies influence the blinking phenomenon, although we cannot rule out that dynamic

properties of O1 assemblies and/or LC interfaces are not changed by the presence of such a high concentration of urea. We note also that additional measurements reported below reveal that amphiphilic assemblies smaller than 250 nm can generate blinks.

Motion of the LC Interface During a Blink. To further characterize the dynamic state of the LC interface during a blink, we tracked the time-dependent locations of tracer particles deposited onto the LC interface. In this experiment, glass microspheres (3 μm in diameter) were dispersed onto the surface of a film of LC in contact with 25 μM O1 in PBS. Fig. 4a-c shows a series of micrographs (polarizers crossed at 30° to enable imaging of the tracer particles) obtained during a blinking event. By tracking the displacements of the glass microspheres, we established that blinking was accompanied by motion of the LC at the interface⁴⁹ (Fig. 4d). The radially directed interfacial flow originated from the center of the blinking event and displaced microspheres up to 100 μm away from the center of the blink. This observation is consistent with a flow driven by a surface pressure gradient that decreases radially from the center of the blinking event.

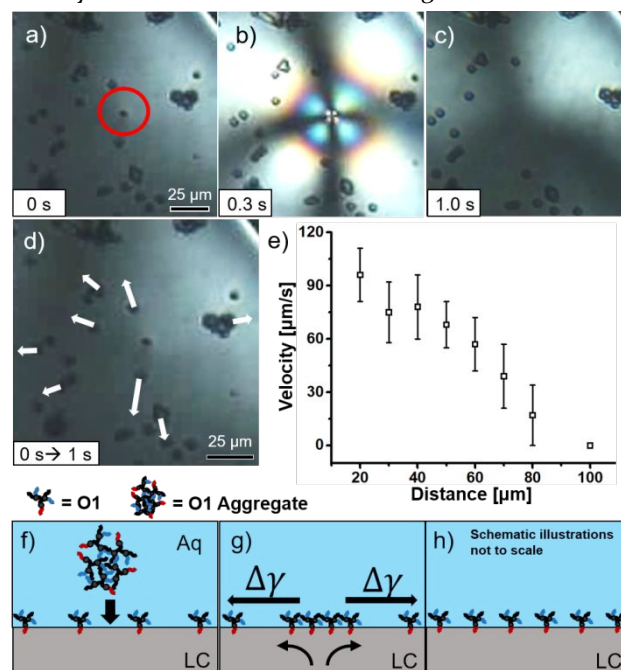


Figure 4: Micrographs of LC films between polarizers crossed at 30° illustrating a) a micrometer-sized O1 aggregate (red circle) above a LC thin film surrounded by glass microspheres (3 μm in diameter), followed by b) a single blinking event and the c) disappearance of the O1 aggregate. The aqueous solution contains 25 μM O1. d) trajectories and e) velocity profile of microspheres as a function of distances stemming radially from the center of a blinking event (n=130, bin size: 10 μm). f-h) Schematic illustrations depicting the mechanism of blinking, showing f) collision of O1 aggregate with LC interface that leads to g) Marangoni flow at the aqueous-LC interface followed by h) rapid spreading of O1 at the LC interface that results in cessation of flow.

We mapped the interfacial flow by analyzing the motion of 130 microspheres (see Materials & Methods). The

microsphere velocities were then plotted against distance from the center of each blinking event (Fig. 4e). As shown in Fig. 4e, the microsphere velocity decreased with increasing distance from the center of the blink. Additionally, we measured the maximum particle velocities to coincide with the peak optical signal from the blink, with particle velocities decreasing with subsequent diminishing optical signal. After the optical signal associated with the blink ceased along with particle motion, a local depletion of tracer particle density was observed in the region of the blink.

We used the above-described measurements of the interfacial velocities of the LC to provide an additional estimate of the tilt angle of the LC induced by the flow accompanying a blink. From Fig. 4e, we calculated the LC surface velocity at a distance of 10 μm from the center of the blinking event ($x=10 \mu\text{m}$) to be $\sim 100 \mu\text{m/s}$. In Section S9, we present a detailed model that evaluates the LC tilt across the film during a blink from a balance of viscous and elastic stresses. This model predicts the average tilt of the LC to be $\theta_{\text{avg}} = 38 \pm 4^\circ$. A similar estimate can be obtained by equating the viscous stress to the elastic torque at the LC-aqueous interface, yielding

$$\alpha_{\text{LC}} (\partial v_x / \partial y) = K_{\text{LC}} (\partial^2 \theta / \partial y^2) \quad (1)$$

where α_{LC} is an effective LC viscosity that is a function of LC tilt (see Section S9 for a more complete analysis), $K_{\text{LC}} \sim 10^{-11} \text{ N}$ is the elastic constant of the LC, v_x is the LC surface velocity, $y \sim 20 \mu\text{m}$ is the LC layer thickness, and θ is the tilt angle of the LC at the aqueous interface.^{9-10, 44, 49} This interfacial stress balance leads to $\theta_{\text{avg}} \sim 35^\circ$. We note that incorporation of internal viscous stresses into our estimate of the LC orientation leads to a larger surface tilt angle than that estimated assuming the LC orientation is dominated by elastic stresses only (see above).

The observations described above, when combined, lead us to propose that each blinking event involves three essential steps. First, an O_1 aggregate in the aqueous phase collides with the aqueous-LC interface (Fig. 4a,f). Second, fusion and adsorption of O_1 molecules from the aggregate with the LC interface generates a lateral O_1 surface concentration gradient. This O_1 surface concentration gradient generates a surface pressure gradient that induces a Marangoni flow away from the collision site (Fig. 4b,g). The shear stress generated by the Marangoni flow is sufficient in magnitude to overcome the elastic torque of the LC, leading the LC to reorient away from the homeotropic orientation.^{38,50-52} The change in LC orientation (and thus optical axis) causes the optical appearance of the LC to change from dark to bright⁴⁹ (Fig. 4b). Third, due to rapid spreading of O_1 across the LC interface, the surface tension gradient dissipates with time and the Marangoni flow ceases. In the absence of flow, the elastic torque of the LC causes the LC to return to the initial perpendicular orientation. The return of the homeotropic LC orientation causes a bright to dark transition in optical appearance (Fig. 4c,h).

Blinking Caused by Vesicles of DLPC. Next we investigated whether LC blinking is observed with amphiphiles other than O_1 . We focused on vesicles formed from the phospholipid DLPC because, unlike O_1 , for which size and concentration of O_1 assemblies are coupled (Fig. 3), the number of lipid vesicles in a dispersion can be controlled by dilution without change of size.^{53, 54} Additionally, the size of DLPC vesicles can be controlled by extrusion through filters containing pores.^{53,55} We also viewed DLPC as a primitive model of biological vesicles, and thus an observation of blinking with DLPC would hint at potential relevance of our observations to studies of vesicle-based events in biological systems.

In our initial experiments with DLPC, films of LC were contacted with aqueous 10 mM PBS containing 100 μM DLPC (as vesicles with diameters of $940 \pm 290 \text{ nm}$; see below for additional characterization). The LCs transitioned to homeotropic orientations after $7 \pm 2 \text{ min}$. These samples, when viewed through crossed polarizers in transmission mode, revealed the presence of blinks with characteristics qualitatively similar to O_1 . Blinking with the DLPC system, however, ceased several minutes after the samples had assumed a homeotropic orientation whereas O_1 -induced blinking continued for hours. Similar to O_1 samples, blinking was observed in DLPC systems prior to (see Section S10) and immediately following the LCs assuming a homeotropic orientation (see Section S11). Quantitative differences in blinking time scales are discussed below.

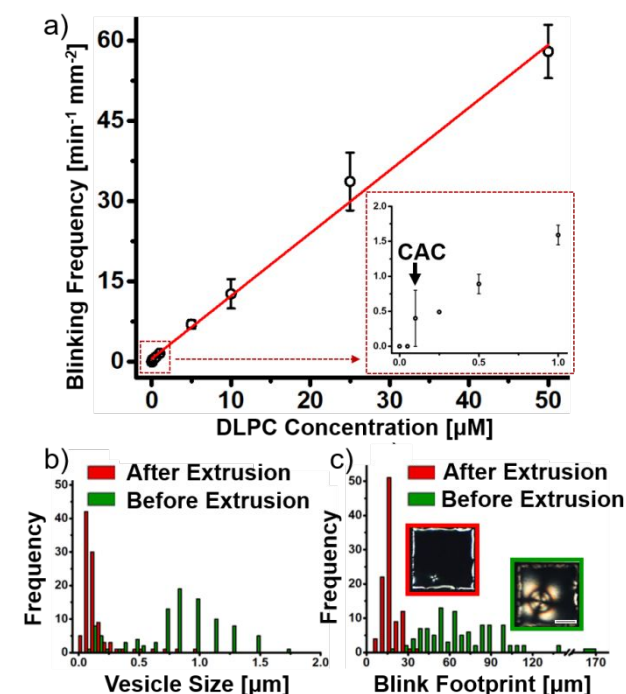


Figure 5: a) Blinking frequency as a function of DLPC concentration in the aqueous solution showing linear relationship. Inset shows magnified plot at low concentrations of DLPC. (b,c) histograms representing (b) number average vesicle diameters before and after extrusion through a 220 nm filter ($n=100$, bin size: 50 nm) and (c) blinking footprints ($n=100$, bin size: 5 μm). Green inset shows large blinking

footprint before vesicle extrusion. Red inset shows small blinking footprint after vesicle extrusion. (c) Scale bar is 100 μm . (a) Data points show mean values and the error bars represent 1 standard deviation ($n=3$).

To understand the relationship between the number of phospholipid vesicles in an aqueous dispersion and blinking frequency, we diluted aqueous dispersions of vesicles (100 μM DLPC stock solution with PBS) to concentrations as low as 0.05 μM DLPC (Fig. 5a). The blinking frequencies were found to be first order in the concentration of DLPC in the dispersion (Fig. 5a). The proportional relationship between blinking frequency and the number of vesicles in the aqueous phase supports our hypothesis that blinking arises from single vesicle collision events. Second, we found that LC blinking occurs at concentrations above but not below 100 nM. Because the critical aggregation concentration (CAC) of DLPC is 100 nM (Fig 5a inset), this result provides further support for our conclusion that blinking is caused by collisions of DLPC vesicles with the LC interface.

We considered it likely that only a small fraction of collisions of vesicles of DLPC with the LC interface generated fusion events and thus blinks. To test this prediction, we performed dynamic light scattering measurements of dispersions of vesicles in aqueous 100 μM DLPC. From the measured average diameters of the vesicles (940 ± 290 nm) and corresponding diffusivities, we estimated that $\sim 10^6$ vesicles collide with a 100 mm^2 area of the LC interface every minute. By using the measured blinking frequency of 47 ± 9 blinks $\text{min}^{-1} \text{mm}^{-2}$, we calculated the probability that a collision between a DLPC vesicle and the LC interface results in fusion and subsequently blinking to be $\sim 10^{-3}$ (see Section S12).

To further explore our proposal that only a small fraction of vesicles colliding with the LC interface subsequently fuse and spread along the interface to cause a blink, we performed measurements using vesicles prepared from lipids conjugated to polyethylene glycol⁵⁶⁻⁵⁸ (DOPE-PEG, Scheme 1d). Consistent with past observations that repulsive steric interactions of PEGylated lipids inhibit spontaneous fusion of liposomes⁵⁸, we did not observe blinking of LC interfaces when using the PEGylated lipid.

Next, we investigated the influence of DLPC vesicle size on LC blinking. We extruded vesicles through a polyvinylidene fluoride (PVDF) filter with a pore diameter of 220 nm and compared the blinking generated by the vesicles before and after extrusion (1 minute after contact between the aqueous DLPC and LC film). To minimize lipid loss during extrusion, we pretreated the filter with 1 mL of aqueous 25 μM DLPC⁵⁹ and the dispersion of DLPC vesicles was passed once through the PVDF filter. We measured the distributions of vesicle sizes (Fig. 5b) and LC optical footprint sizes, both before and after extrusion of the vesicles (Fig. 5c). Prior to vesicle extrusion, the vesicle and blinking footprint diameters were 800 ± 80 nm and 70 ± 5 μm , respectively, whereas following extrusion, they decreased to 150 ± 30 nm and 20 ± 1 μm , respectively (95%

confidence interval, see Section S13). Overall, this result and others presented below establish that a decrease in vesicle size correlates with a decrease in blinking footprint size. This result hints at the utility of blinking as a means of probing heterogeneity in a population of vesicles (or other amphiphilic assemblies) at the single vesicle level.

Guided by the result above that blinking footprint size correlates with vesicle size, we explored changes in blinking that accompany vesicle destruction in mixed lipid/surfactant systems. Here, the aqueous solution comprised mixtures of DTAB and DLPC, resulting in the formation of mixed DTAB/DLPC assemblies. Dynamic light scattering measurements of DLPC and DTAB mixtures confirmed a decrease in assembly size with increasing DTAB concentrations (see Section S14). Concurrent with the change in vesicle size, the blinking footprint also decreased. However, we observed a complex relationship between blinking frequency and DTAB concentration, which we do not yet fully understand but suspect reflects competitive dynamics of DTAB and DLPC adsorption and spreading at the LC interface.

Comparison of Blinking with O₁ and DLPC. The results above establish that blinking is observed with both O₁ assemblies and vesicles of DLPC. We note, however, that key differences were observed between these two systems. In particular, as shown in Fig. 6, O₁-induced blinking at LC interfaces is sustained for hours, whereas DLPC-triggered blinking persists for ~ 10 -15 mins after contact of the LC with the dispersion of amphiphiles. The duration over which LC blinking with DLPC is observed is consistent with the time scale required for the LC interface to saturate with the phospholipid (~ 15 mins).⁶⁰ The long duration over which O₁ is observed to generate blinks, however, suggests that an additional mechanism must be active to prevent saturation of the LC interface with O₁ after a few minutes. Additionally, in contrast to DLPC, inspection of Fig. 6 reveals that O₁ exhibits a local minimum in blinking frequency with incubation time.

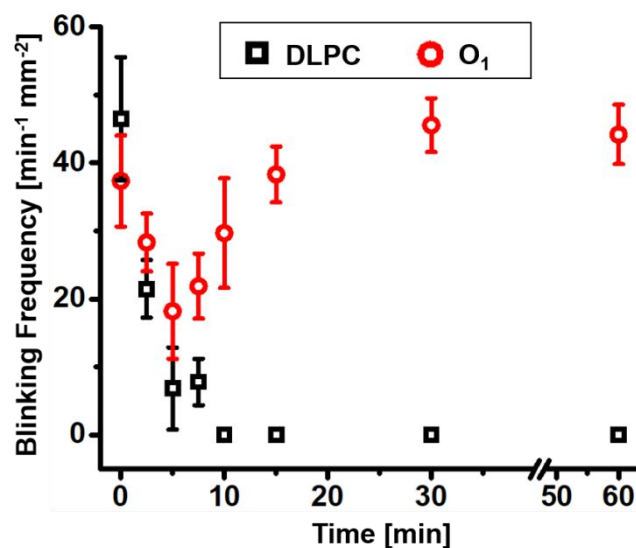


Figure 6: Blinking frequency as a function of time for LC thin films in contact with an aqueous solution containing 100 μM DLPC (black squares) and 25 μM O_1 (red circles). Data points show mean values and the error bars represent 1 standard deviation ($n=3$).

We hypothesized that blinking by O_1 was sustained for hours by desorption of O_1 from the LC interface into the LC bulk, thus enabling further collisions and spreading of O_1 aggregates from the aqueous solution onto the interface. Several observations support this hypothesis. First, we measured the temperature at which the 5CB transitioned from a nematic to an isotropic phase (T_{NI}) to change following incubation with O_1 but not DLPC, consistent with desorption of O_1 but not DLPC into the LC bulk (see Section S15). Second, we determined that pre-loading O_1 into 5CB suppressed blinking upon incubation of the 5CB against an aqueous dispersion of O_1 . This result is consistent with the presence of O_1 in the LC bulk decreasing the rate of desorption of O_1 from the interface into the LC bulk, thus slowing the rate of blinking (see Section S15).

Additional support for the hypothesized role of O_1 desorption into the LC bulk was obtained by incubating a LC film against a 25 μM O_1 aqueous solution for 24 hours. Between crossed polarizers, we observed a $\sim 80\%$ decrease in blinking frequency after 24 hrs. We note, however, that while we conclude that sustained blinking is enabled by O_1 desorption (see Section S15), we do not yet understand why O_1 exhibits a local minimum in blinking frequency after 5 mins (Fig. 6). Additional studies are needed to elucidate the complex kinetics associated with O_1 blinking. Our results, however, clearly establish that blinking is a consequence of a delicate interplay of O_1 adsorption from the aqueous bulk onto the LC interface, and desorption of O_1 from the interface into the LC bulk.

CONCLUSIONS

In conclusion, this paper reports that dynamic, non-equilibrium interfacial states of LCs can be triggered by interactions with individual supramolecular assemblies of amphiphilic molecules with the LC interface. We have discovered reversible, spatially localized, sub-second transitions in LC orientation that arise from collisions of single amphiphilic assemblies dispersed in aqueous solution with the LC interface. Collision and subsequent rapid spreading of amphiphiles along the LC interface give rise to a surface tension gradient that triggers transient and localized interfacial (Marangoni) flows. The Marangoni flows realign the LC, inducing a localized change in the optical appearance of the LC (a “blink”).^{38, 51-52} Due to the rapid spreading of amphiphiles at the LC interface, the interfacial tension gradient dissipates within seconds, causing flow to cease and thereby allowing the LC to relax to its equilibrium orientation. We conclude that some amphiphiles (O_1) in our study desorb from the LC interface into the LC, thus enabling further adsorption of amphiphilic assemblies, leading to blinking that is sustained over hours.

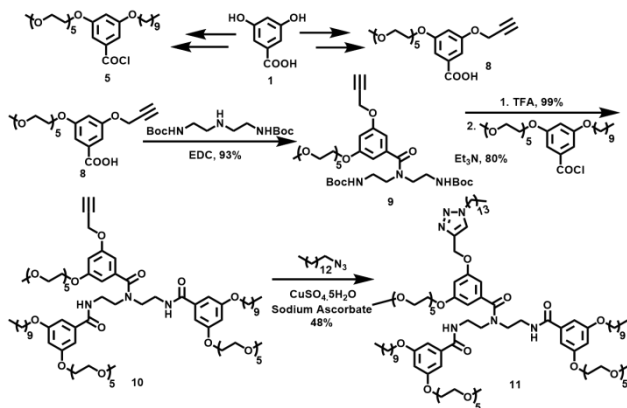
The observations reported in this paper generate a number of interesting questions. For example, we infer that the fraction of vesicles of DLPC colliding with the LC interface that generate a blink to be approximately 10^{-3} . Additional studies are needed to fully understand the factors that control this sticking probability, although we predict that it will depend strongly on the properties of the amphiphiles within their assemblies⁶¹⁻⁶² (e.g., LC or gel-like state of phospholipids within bilayers). We also do not yet understand how the properties of the LC impact the collision, interactions and spreading of amphiphilic assemblies (e.g., LC dynamic rheological properties and interfacial properties such as charge). We envisage that ionic strength,⁶³⁻⁶⁵ pH⁶⁶⁻⁶⁹ and viscosity⁷⁰⁻⁷⁴ of the aqueous phase will play a key role in regulating the interactions of vesicles with the LC interface.³² Additionally, Marangoni stresses at the aqueous-LC interface during a blinking event will generate localized flow in the aqueous phase, which in turn may facilitate the transfer of amphiphilic assemblies from the aqueous bulk onto the LC interface. Finally, although we establish that the sizes of DLPC vesicles impact the characteristic features of the blinks (footprint), the lower limit to vesicle size that generates a measurable blink is unknown.

The results in this paper also suggest a range of future directions of inquiry, such as determining if biologically-derived vesicles (e.g., exosomes) induce blinking of LCs. This direction of investigation has the potential to yield important results as variations in composition of vesicles shed from eukaryotic cells in biological systems can provide key information regarding cell health.^{3, 75} Such studies may offer the basis of novel analytical methods for detecting and characterizing microvesicles. It is also possible that the system reported in this paper might be used to screen for peptides, other additives (e.g., ions) or molecular recognition groups that facilitate fusion of vesicles at interfaces. These and other ideas building from the study reported in this paper will be described in future publications.

MATERIALS AND METHODS

Materials. The nematic LC 4-cyano-4'-pentylbiphenyl (5CB) was purchased from HCH (Jiangsu Hecheng Display Technology Co., Ltd). Fisher Finest Premium Grade glass slides were purchased from Fisher Scientific (Pittsburgh, PA). N,N-dimethyl-N-octadecyl-3-aminopropyltrimethoxysilylchloride (DMOAP) was purchased from Acros Organics. Purification of water (18.2 M Ω cm resistivity at 25 $^{\circ}\text{C}$) was performed using a Milli-Q water system (Millipore, Bedford, MA, USA). DLPC was purchased from Avanti (Alabaster, AL, USA).

Synthesis of O_1 .



Scheme 2: Synthetic pathway of O₁.

O₁, **11** (Scheme 2), was synthesized via a 13-step synthetic protocol from 3, 5-dihydroxy benzoic acid, **1**. We have previously reported the synthesis of **5** and **8** from **1**³². Using **8**, **9** was synthesized via N-(3-Dimethylaminopropyl)-N-ethylcarbodiimide hydrochloride (EDC-HCl) coupling between the alkyne **8** and di-tert-butyl (azanediylbis(ethane-2,1-diyl)) dicarbamate with a yield of 93%. Following this reaction, **10** was synthesized at 80% yield via a 2-step protocol by first deprotecting tert-butyloxycarbonyl and its subsequent substitution reaction with **5**. The final step involved a copper-click reaction between **10** and tetradecane azide to synthesize O₁ at 48% yield. The characteristic peak of the propargyl group at 3.08 ppm disappears and a peak corresponding to triazole proton at 7.61 ppm arises in ¹H NMR, indicating the successful alkyne-azide coupling. All compounds in this scheme were characterized via ¹H, ¹³C NMR and ESI-MS spectroscopy. Details of the synthesis of O₁ are provided in SI.

Preparation of Thin LC Films. Thin films of 5CB were prepared by pipetting 0.5 μL of 5CB into the pores of 75 mesh (thickness 20 μm; lateral pore size 285 μm) transmission electron microscopy (TEM) grids supported on a DMOAP-functionalized glass substrate (Details of DMOAP functionalization are provided in SI). Excess 5CB was then removed to produce a LC film with thickness of 20 μm.

Microscopy Observations. An Olympus BX41 microscope with 4x, 20x and 50x objectives, two rotating polarizers and a Moticam 10.0 MP camera was used for optical microscopy.

Determination of Blinking Frequency. Blinking frequencies were measured by observing the optical response of nine TEM grid squares (285 μm x 285 μm) filled with LC. For measurements with O₁, we recorded the numbers of blinks over a 1 minute interval approximately 55 min, 60 min or 65 min after contact of the LC film with the aqueous O₁ dispersion. Individual blinking events were identified by examining frames of videos. The blinking events recorded during each of the 1 minute intervals were averaged and used as one independent measurement. Three independent measurements were averaged to obtain each average blinking rate reported in this paper. The average blinking frequencies were then divided by the LC

surface area defined by the nine TEM grids (0.731 mm²) and plotted as a function of concentration. Unless otherwise specified, blinking frequencies generated by DLPC vesicles were determined 1 minute after contact of the LC with aqueous DLPC dispersions.

Dynamic Light Scattering. 1 mL of desired concentrations of O₁ (0-25 μM) in PBS were prepared in glass tubes from a 100 μM O₁ stock solution and allowed to incubate for 4 hours at 25 °C. Following incubation, dynamic light scattering measurements (Brookhaven Instrument) at 25 °C were recorded at four different light scattering angles (75°, 90°, 110° and 140°) and the corresponding autocorrelation functions were normalized using the Siegert relationship.⁷⁶⁻⁷⁷ The normalized autocorrelation functions for each concentration of O₁ were then rescaled⁷⁶ to determine whether the measured sizes of O₁ aggregates in the aqueous solution were true hydrodynamic diameters. A similar methodology was used to determine the sizes of the dispersions of DLPC vesicles.

Particle Tracking at LC Interfaces. The positions of 130 glass microspheres (3 μm diameter) dispersed at the aqueous-LC interface were recorded by video (30 ms/frame) during blinking events. The velocities were calculated from the videos and plotted as a function of distance of each microsphere from the center of each blink.

Safety Statement: No unexpected or unusually high safety hazards were encountered.

ASSOCIATED CONTENT

Supporting Information

Mechanism of LC reorientation (Section S1); Calculation of O₁ aggregate diffusion time (Section S2); LC tilt estimate during a blinking event (Section S3); Blinking using bright field microscopy (Section S4); O₁-induced blinking at planar/tilted LC interfaces (Section S5); Role of O₁ aggregates in blinking (Section S6); Dynamic light scattering from aq O₁ solutions (Section S7); Disruption of O₁ aggregates with urea (Section S8); Theoretical estimate of LC tilt from a stress balance (Section S9); DLPC-induced blinking at LC interfaces with planar/tilted alignment (Section S10); DLPC-induced blinking at LC interfaces with homeotropic alignment (Section S11); Estimation of fusion probability as reported by blinking (Section S12); Vesicle extrusion (Section S13); Disruption of lipid vesicles by DTAB (Section S14); Desorption of amphiphiles into the bulk LC (Section S15); Methods for preparation of O₁ aq dispersions, DMOAP-functionalization of glass slides, and preloading LC with O₁; Methods for synthetic pathways, procedures and characterization of O₁; Movie of blinking (Video S1)

AUTHOR INFORMATION

Corresponding Author

*E-mail: thai@chem.umass.edu

*E-mail: nabbott@cornell.edu

Author Contributions

[†]These authors contributed equally to this work.

Notes

The authors declare no competing financial interest

ACKNOWLEDGEMENTS

We acknowledge support of this research from the Army Research Office through W911NF-15-1-0568 and W911NF-17-1-0575. The authors also thank Hector Fuster and Karthik Nayani for their helpful comments on this work.

REFERENCES

- (1) Lentz, B. R.; Malinin, V.; Haque, M. E.; Evans, K. Protein Machines and Lipid Assemblies: Current Views of Cell Membrane Fusion. *Curr. Opin. Struc. Biol.* **2000**, *10* (5), 607-615.
- (2) Lee, Y.; El Andaloussi, S.; Wood, M. J. A. Exosomes and Microvesicles: Extracellular Vesicles for Genetic Information Transfer and Gene Therapy. *Hum. Mol. Genet.* **2012**, *21*, R125-R134.
- (3) Muralidharan-Chari, V.; Clancy, J. W.; Sedgwick, A.; D'Souza-Schorey, C. Microvesicles: Mediators of Extracellular Communication During Cancer Progression. *J. Cell Sci.* **2010**, *123* (10), 1603-1611.
- (4) Saheki, Y.; De Camilli, P. Synaptic Vesicle Endocytosis. *Cold Spring Harb. Perspect. Biol.* **2012**, *4* (9), a005645.
- (5) Duzgunes, N. Fluorescence Assays for Liposome Fusion. *Methods Enzymol.* **2003**, *372*, 260-274.
- (6) Knoll, W.; Park, H.; Sinner, E. K.; Yao, D. F.; Yu, F. Supramolecular Interfacial Architectures for Optical Biosensing with Surface Plasmons. *Surf. Sci.* **2004**, *570* (1-2), 30-42.
- (7) Jackson, B. L.; Groves, J. T. Scanning Probe Lithography on Fluid Lipid Membranes. *J. Am. Chem. Soc.* **2004**, *126* (43), 13878-13879.
- (8) Chen, X. Y.; Chen, Z. SFG Studies on Interactions between Antimicrobial Peptides and Supported Lipid Bilayers. *Biochim. Biophys. Acta—Biomembranes* **2006**, *1758* (9), 1257-1273.
- (9) Kléman, M.; Lavrentovich, O. D. *Soft Matter Physics: an Introduction*. Springer: New York, 2003.
- (10) Gennes, P. G. d.; Prost, J. *The Physics of Liquid Crystals*. 2nd ed.; Clarendon Press; Oxford University Press: Oxford New York, 1993.
- (11) Popov, P.; Mann, E. K.; Jakli, A. Thermotropic Liquid Crystal Films for Biosensors and Beyond. *J. Mater. Chem. B* **2017**, *5* (26), 5061-5078.
- (12) Bukusoglu, E.; Pantoja, M. B.; Mushenheim, P. C.; Wang, X. G.; Abbott, N. L. Design of Responsive and Active (Soft) Materials Using Liquid Crystals. *Annu. Rev. Chem. Biomol.* **2016**, *7*, 163-196.
- (13) Carlton, R. J.; Hunter, J. T.; Miller, D. S.; Abbasi, R.; Mushenheim, P. C.; Tan, L. N.; Abbott, N. L. Chemical and Biological Sensing Using Liquid Crystals. *Liq. Cryst. Rev.* **2013**, *1* (1), 29-51.
- (14) Miller, D. S.; Wang, X. G.; Abbott, N. L. Design of Functional Materials Based on Liquid Crystalline Droplets. *Chem. Mater.* **2014**, *26* (1), 496-506.
- (15) Kim, Y. K.; Huang, Y.; Tsuei, M.; Wang, X.; Gianneschi, N. C.; Abbott, N. L. Multi-Scale Responses of Liquid Crystals Triggered by Interfacial Assemblies of Cleavable Homopolymers. *ChemPhysChem* **2018**, *19* (16), 2037-2045.
- (16) Gelebart, A. H.; Mulder, D. J.; Varga, M.; Konya, A.; Vantomme, G.; Meijer, E. W.; Selinger, R. L. B.; Broer, D. J. Making Waves in a Photoactive Polymer Film. *Nature* **2017**, *546* (7660), 632-636.
- (17) Wang, Y.; Li, Q. Light-Driven Chiral Molecular Switches or Motors in Liquid Crystals. *Adv. Mater.* **2012**, *24* (15), 1926-1945.
- (18) Liu, Y. Y.; Wu, W.; Wei, J.; Yu, Y. L. Visible Light Responsive Liquid Crystal Polymers Containing Reactive Moieties with Good Processability. *ACS Appl. Mater. Interfaces* **2017**, *9* (1), 782-789.
- (19) Paterson, D. A.; Xiang, J.; Singh, G.; Walker, R.; Agra-Kooijman, D. M.; Martinez-Felipe, A.; Gan, M.; Storey, J. M. D.; Kumar, S.; Lavrentovich, O. D.; Imrie, C. T. Reversible Isothermal Twist-Bend Nematic-Nematic Phase Transition Driven by the Photoisomerization of an Azobenzene-Based Nonsymmetric Liquid Crystal Dimer. *J. Am. Chem. Soc.* **2016**, *138* (16), 5283-5289.
- (20) Cox, J. R.; Simpson, J. H.; Swager, T. M. Photoalignment Layers for Liquid Crystals from the Di- π -methane Rearrangement. *J. Am. Chem. Soc.* **2013**, *135* (2), 640-643.
- (21) Adamiak, L.; Pendery, J.; Sun, J. W.; Iwabata, K.; Gianneschi, N. C.; Abbott, N. L. Design Principles for Triggerable Polymeric Amphiphiles with Mesogenic Side Chains for Multiscale Responses with Liquid Crystals. *Macromolecules* **2018**, *51* (5), 1978-1985.
- (22) Zhou, J. S.; Dong, Y. C.; Zhang, Y. Y.; Liu, D. S.; Yang, Z. Q. The Assembly of DNA Amphiphiles at Liquid Crystal-Aqueous Interface. *Nanomaterials* **2016**, *6* (12), 229.
- (23) Wang, X.; Yang, P.; Mondiot, F.; Li, Y.; Miller, D. S.; Chen, Z.; Abbott, N. L. Interfacial Ordering of Thermotropic Liquid Crystals Triggered by the Secondary Structures of Oligopeptides. *Chem. Commun. (Cambridge, U.K.)* **2015**, *51* (94), 16844-16847.
- (24) Daschner De Tercero, M.; Abbott, N. L. Ordering Transitions in Liquid Crystals Permit Imaging of Spatial and Temporal Patterns Formed by Proteins Penetrating into Lipid-Laden Interfaces. *Chem. Eng. Commun.* **2008**, *196* (1-2), 234-251.
- (25) Szilvasi, T.; Bao, N. Q.; Yu, H. Z.; Twieg, R. J.; Mavrikakis, M.; Abbott, N. L. The Role of Anions in Adsorbate-induced Anchoring Transitions of Liquid Crystals on Surfaces with Discrete Cation Binding Sites. *Soft Matter* **2018**, *14* (5), 797-805.
- (26) Carlton, R. J.; Ma, C. D.; Gupta, J. K.; Abbott, N. L. Influence of Specific Anions on the Orientational Ordering of Thermotropic Liquid Crystals at Aqueous Interfaces. *Langmuir* **2012**, *28* (35), 12796-12805.
- (27) Brake, J. M.; Daschner, M. K.; Abbott, N. L. Formation and Characterization of Phospholipid Monolayers Spontaneously Assembled at Interfaces between Aqueous Phases and Thermotropic Liquid Crystals. *Langmuir* **2005**, *21* (6), 2218-2228.
- (28) Brake, J. M.; Daschner, M. K.; Luk, Y. Y.; Abbott, N. L. Biomolecular Interactions at Phospholipid-decorated Surfaces of Liquid Crystals. *Science* **2003**, *302* (5653), 2094-2097.
- (29) Brake, J. M.; Mezera, A. D.; Abbott, N. L. Effect of Surfactant Structure on the Orientation of Liquid Crystals at Aqueous-liquid Crystal Interfaces. *Langmuir* **2003**, *19* (16), 6436-6442.
- (30) Tian, T. T.; Kang, Q.; Wang, T.; Xiao, J. H.; Yu, L. Alignment of Nematic Liquid Crystals Decorated with Gemini Surfactants and Interaction of Proteins with Gemini

- Surfactants at Fluid Interfaces. *J. Colloid Interface Sci.* **2018**, *518*, 111-121.
- (31) Concellon, A.; Zentner, C. A.; Swager, T. M. Dynamic Complex Liquid Crystal Emulsions. *J. Am. Chem. Soc.* **2019**, *141* (45), 18246-18255.
- (32) Kim, Y. K.; Raghupathi, K. R.; Pendery, J. S.; Khomein, P.; Sridhar, U.; Pablo, J. J.; Thayumanavan, S.; Abbott, N. L. Oligomers as Triggers for Responsive Liquid Crystals. *Langmuir* **2018**, *34* (34), 10092-10101.
- (33) Lockwood, N. A.; de Pablo, J. J.; Abbott, N. L. Influence of Surfactant Tail Branching and Organization on the Orientation of Liquid Crystals at Aqueous-liquid Crystal Interfaces. *Langmuir* **2005**, *21* (15), 6805-6814.
- (34) Lowe, A. M.; Abbott, N. L. Liquid Crystalline Materials for Biological Applications. *Chem. Mater.* **2012**, *24* (5), 746-758.
- (35) Badami, J. V.; Bernstein, C.; Maldarelli, C.; Tu, R. S. Adsorption of Rationally Designed "Surf-tides" to a Liquid-Crystal Interface. *Soft Matter* **2015**, *11* (33), 6604-6612.
- (36) Ramezani-Dakhel, H.; Rahimi, M.; Pendery, J.; Kim, Y. K.; Thayumanavan, S.; Roux, B.; Abbott, N. L.; de Pablo, J. J. Amphiphile-Induced Phase Transition of Liquid Crystals at Aqueous Interfaces. *ACS Appl. Mater. Interfaces* **2018**, *10* (43), 37618-37624.
- (37) Carlton, R. J.; Gupta, J. K.; Swift, C. L.; Abbott, N. L. Influence of Simple Electrolytes on the Orientational Ordering of Thermotropic Liquid Crystals at Aqueous Interfaces. *Langmuir* **2012**, *28* (1), 31-36.
- (38) Choi, H.; Takezoe, H. Circular Flow Formation Triggered by Marangoni Convection in Nematic Liquid Crystal Films with a Free Surface. *Soft Matter* **2016**, *12* (2), 481-485.
- (39) Jeong, J.; Gross, A.; Wei, W. S.; Tu, F. Q.; Lee, D.; Collings, P. J.; Yodh, A. G. Liquid Crystal Janus Emulsion Droplets: Preparation, Tumbling, and Swimming. *Soft Matter* **2015**, *11* (34), 6747-6754.
- (40) Heo, P.; Yang, Y.; Han, K. Y.; Kong, B.; Shin, J. H.; Jung, Y.; Jeong, C.; Shin, J.; Shin, Y. K.; Ha, T.; Kweon, D. H. A Chemical Controller of SNARE-Driven Membrane Fusion That Primes Vesicles for Ca²⁺-Triggered Millisecond Exocytosis. *J. Am. Chem. Soc.* **2016**, *138* (13), 4512-4521.
- (41) Yang, J.; Bahreman, A.; Daudey, G.; Bussmann, J.; Olsthoorn, R. C. L.; Kros, A. Drug Delivery via Cell Membrane Fusion Using Lipopeptide Modified Liposomes. *ACS Central Sci.* **2016**, *2* (9), 621-630.
- (42) Tan, L. N.; Orler, V. J.; Abbott, N. L. Ordering Transitions Triggered by Specific Binding of Vesicles to Protein-Decorated Interfaces of Thermotropic Liquid Crystals. *Langmuir* **2012**, *28* (15), 6364-6376.
- (43) Kuhlmann, J. W.; Junius, M.; Diederichsen, U.; Steinem, C. SNARE-Mediated Single-Vesicle Fusion Events with Supported and Freestanding Lipid Membranes. *Biophys. J.* **2017**, *113* (11), 2573-2574.
- (44) Kim, Y. K.; Wang, X. G.; Mondkar, P.; Bukusoglu, E.; Abbott, N. L. Self-reporting and Self-regulating Liquid crystals. *Nature* **2018**, *557* (7706), 539-544.
- (45) Yang, D.-K.; Wu, S.-T. Fundamentals of Liquid Crystal Devices. John Wiley: Chichester ; Hoboken, NJ, 2006, 378.
- (46) Hua, L.; Zhou, R. H.; Thirumalai, D.; Berne, B. J. Urea Denaturation by Stronger Dispersion Interactions with Proteins than Water Implies a 2-stage Unfolding. *Proc. Natl. Acad. Sci. U.S.A.* **2008**, *105* (44), 16928-16933.
- (47) Klimov, D. K.; Straub, J. E.; Thirumalai, D. Aqueous Urea Solution Destabilizes A β_{16-22} Oligomers. *Proc. Natl. Acad. Sci. U.S.A.* **2004**, *101* (41), 14760-14765.
- (48) Wang, W.; Roberts, C. J. Aggregation of Therapeutic Proteins. Wiley: Hoboken, N.J., 2010.
- (49) Kim, Y. K.; Senyuk, B.; Lavrentovich, O. D. Molecular Reorientation of a Nematic Liquid Crystal by Thermal Expansion. *Nature Communications* **2012**, *3*, 1133-1139.
- (50) Kruger, C.; Klos, G.; Bahr, C.; Maass, C. C. Curling Liquid Crystal Microswimmers: A Cascade of Spontaneous Symmetry Breaking. *Phys. Rev. Lett.* **2016**, *117* (4), No. 048003.
- (51) Herminghaus, S.; Maass, C. C.; Kruger, C.; Thutupalli, S.; Goehring, L.; Bahr, C. Interfacial Mechanisms in Active Emulsions. *Soft Matter* **2014**, *10* (36), 7008-7022.
- (52) Maass, C. C.; Kruger, C.; Herminghaus, S.; Bahr, C. Swimming Droplets. *Annu. Rev. Condens. Matter Phys.* **2016**, *7*, 171-193.
- (53) Hunter, D. G.; Frisken, B. J. Effect of Extrusion Pressure and Lipid Properties on the Size and Polydispersity of Lipid Vesicles. *Biophys. J.* **1998**, *74* (6), 2996-3002.
- (54) Schurtenberger, P.; Mazer, N.; Waldvogel, S.; Kanzig, W. Preparation of Monodisperse Vesicles with Variable Size by Dilution of Mixed Micellar Solutions of Bile-Salt and Phosphatidylcholine. *Biochim. Biophys. Acta* **1984**, *775* (1), 111-114.
- (55) Mayer, L. D.; Hope, M. J.; Cullis, P. R. Vesicles of Variable Sizes Produced by a Rapid Extrusion Procedure. *Biochim. Biophys. Acta* **1986**, *858* (1), 161-168.
- (56) Yang, Z. Q.; Gupta, J. K.; Kishimoto, K.; Shoji, Y.; Kato, T.; Abbott, N. L. Design of Biomolecular Interfaces Using Liquid Crystals Containing Oligomeric Ethylene Glycol. *Adv. Funct. Mater.* **2010**, *20* (13), 2098-2106.
- (57) Li, L. Y.; Chen, S. F.; Zheng, J.; Ratner, B. D.; Jiang, S. Y. Protein Adsorption on Oligo(ethylene glycol)-terminated Alkanethiolate Self-assembled Monolayers: The Molecular Basis for Nonfouling Behavior. *J. Phys. Chem. B.* **2005**, *109* (7), 2934-2941.
- (58) Noonan, P. S.; Mohan, P.; Goodwin, A. P.; Schwartz, D. K. DNA Hybridization-Mediated Liposome Fusion at the Aqueous Liquid Crystal Interface. *Adv. Funct. Mater.* **2014**, *24* (21), 3206-3212.
- (59) Fayolle, D.; Fiore, M.; Stano, P.; Strazewski, P. Rapid Purification of Giant Lipid Vesicles by Microfiltration. *PLoS ONE* **2018**, *13* (2): e0192975.
- (60) Lockwood, N. A.; Abbott, N. L. Self-assembly of Surfactants and Phospholipids at Interfaces between Aqueous Phases and Thermotropic Liquid Crystals. *Curr. Opin. Colloid Interface Sci.* **2005**, *10* (3-4), 111-120.
- (61) Leckband, D. E.; Helm, C. A.; Israelachvili, J. Role of Calcium in the Adhesion and Fusion of Bilayers. *Biochemistry* **1993**, *32* (4), 1127-1140.
- (62) Wieland, J. A.; Gewirth, A. A.; Leckband, D. E. Single-molecule Measurements of the Impact of Lipid Phase Behavior on Anchor Strengths. *J. Phys. Chem. B.* **2005**, *109* (12), 5985-5993.
- (63) Kadima, W.; Ogendal, L.; Bauer, R.; Kaarsholm, N.; Brodersen, K.; Hansen, J. F.; Porting, P. The Influence of Ionic Strength and pH on the Aggregation Properties of Zinc-free Insulin Studied by Static and Dynamic Laser Light Scattering. *Biopolymers* **1993**, *33* (11), 1643-1657.
- (64) French, R. A.; Jacobson, A. R.; Kim, B.; Isley, S. L.; Penn, R. L.; Baveye, P. C. Influence of Ionic Strength, pH, and Cation Valence on Aggregation Kinetics of Titanium Dioxide Nanoparticles. *Environ. Sci. Technol.* **2009**, *43* (5), 1354-1359.
- (65) Wang, L. X.; Yang, X. Z.; Wang, Q.; Zeng, Y. X.; Ding, L.; Jiang, W. Effects of Ionic Strength and Temperature on the

- Aggregation and Deposition of Multi-walled Carbon Nanotubes. *J. Environ. Sci.* **2017**, 51, 248-255.
- (66) Li, R.; Wu, Z.; Wangb, Y.; Ding, L.; Wang, Y. Role of pH-Induced Structural Change in Protein Aggregation in Foam Fractionation of Bovine Serum Albumin. *Biotechnol. Rep.* **2016**, 9, 46-52.
- (67) Wang, W. Protein Aggregation and its Inhibition in Biopharmaceutics. *Int. J. Pharm.* **2005**, 289 (1-2), 1-30.
- (68) Cromwell, M. E.; Hilario, E.; Jacobson, F. Protein Aggregation and Bioprocessing. *AAPS J.* **2006**, 8 (3), E572-579.
- (69) Engelhardt, K.; Lexis, M.; Gochev, G.; Konnerth, C.; Miller, R.; Willenbacher, N.; Peukert, W.; Braunschweig, B. pH Effects on the Molecular Structure of Beta-lactoglobulin Modified Air-water Interfaces and its Impact on Foam Rheology. *Langmuir* **2013**, 29 (37), 11646-11655.
- (70) Loudet, J. C.; Hanusse, P.; Poulin, P. Stokes Drag on a Sphere in a Nematic Liquid Crystal. *Science* **2004**, 306 (5701), 1525-1525.
- (71) Crocker, J. C.; Hoffman, B. D. Multiple-particle Tracking and Two-point Microrheology in Cells. *Methods Cell Biol.* **2007**, 83, 141-178.
- (72) Crocker, J. C.; Valentine, M. T.; Weeks, E. R.; Gisler, T.; Kaplan, P. D.; Yodh, A. G.; Weitz, D. A. Two-point Microrheology of Inhomogeneous Soft Materials. *Phys. Rev. Lett.* **2000**, 85 (4), 888-891.
- (73) Sleutel, M.; Van Driessche, A. E. S.; Pan, W. C.; Reichel, E. K.; Maes, D.; Vekilov, P. G. Does Solution Viscosity Scale the Rate of Aggregation of Folded Proteins? *J. Phys. Chem. Lett.* **2012**, 3 (10), 1258-1263.
- (74) Ansari, A.; Jones, C. M.; Henry, E. R.; Hofrichter, J.; Eaton, W. A. The Role of Solvent Viscosity in the Dynamics of Protein Conformational Changes. *Science* **1992**, 256 (5065), 1796-1798.
- (75) Al-Nedawi, K.; Meehan, B.; Rak, J. Microvesicles Messengers and Mediators of Tumor Progression. *Cell Cycle* **2009**, 8 (13), 2014-2018.
- (76) Stetefeld, J.; McKenna, S. A.; Patel, T. R. Dynamic Light Scattering: a Practical Guide and Applications in Biomedical Sciences. *Biophys. Rev.* **2016**, 8 (4), 409-427.
- (77) Voigt, H.; Hess, S. Comparison of the Intensity Correlation-Function and the Intermediate Scattering Function of Fluids: a Molecular Dynamics Study of the Siegert Relation. *Physica A* **1994**, 202 (1-2), 145-164.

